3D atherosclerotic plaque distribution in the Western diet-fed PCSK9-AAV mouse model of atherosclerosis

Authors

Urmas Roostalu, Ditte Marie-Jensen, Casper Gravesen Salinas, Sheyla Barrado Ballestero, Jacob Lercke Skytte, Henrik H. Hansen, Michael Christensen

Gubra, Hørsholm, Denmark

Contact: Michael Christensen mch@gubra.dk

BACKGROUND & AIM

Complications of atherosclerosis remain the leading cause of morbidity and mortality worldwide. Proprotein-convertase-subtilisin/kexin type 9 (PCSK9) function is associated with reduced clearance of circulating LDL-cholesterol, a key risk factor for developing atherosclerosis and therefore also an important drug target.

The present study aimed to assess progression of dyslipidemia and aortic atherosclerotic lesions facilitated by adeno-associated virus (AAV)-mediated overexpression of PCSK9 in diet-induced obese (DIO-PCSK9-AAV) mice.

METHODS

Male C57Bl/6J mice were made diet-induced obese (DIO) by feeding a Western diet (#D12079B Research diets, 41% fat-kcal, 0.21% cholesterol) for 12 or 17 weeks, respectively. Chow-fed mice served as controls. At study start, all mice received a single tail vein injection of murine PCSK9-AAV. Terminal endpoints included body weight, plasma markers of dyslipidemia (HDL/LDL-cholesterol, total cholesterol, triglycerides) and aortic atherogenic plaque load. Aortic branch whole-mounts were stained for CD45+ immune cells (leukocytes), cleared and imaged using 3D light sheet microscopy. Deep learning computational analysis was applied for rapid detection, mapping and quantification of atherogenic plaques (autofluorescence) and CD45+ leukocyte infiltrates in the vascular wall.

www.gubra.dk

1 Study outline

Group	Dose (GC)	Study duration	Diet	Number of animals
1	Chow-PCSK9-AAV 17 wks	1.0×10^{11}	17 weeks	Chow	11
2	DIO-PCSK9-AAV 12 wks	1.0×10^{11}	12 weeks	Western diet	14
3	DIO-PCSK9-AAV 17 wks	1.0×10^{11}	17 weeks	Western diet	14

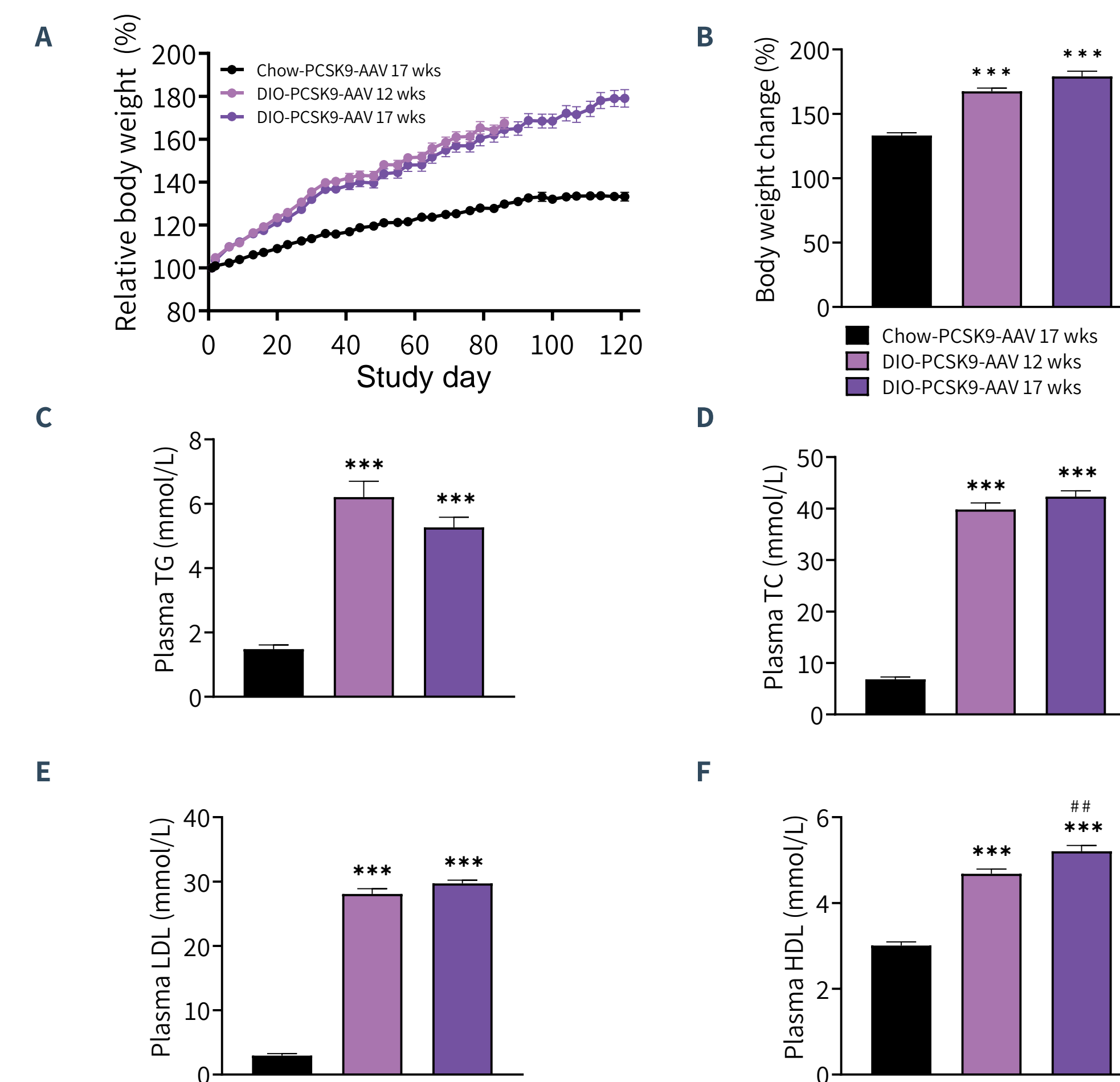## 2 Metabolic and plasma lipid parameters

Figure 1. DIO-PCSK9-AAV mice demonstrate dyslipidemia, including marked LDL-hypercholesterolemia. (A) Body weight change relative to baseline (day 1). (B) Terminal body weight change compared to baseline (Day 1, %). (C-F) Terminal plasma markers of dyslipidimia. (C) Triglycerides (TG). (D) Total cholesterol (TC). (E) Low-density lipoprotein (LDL)-cholesterol. (F) High-density lipoprotein (HDL)-cholesterol. ***$p<0.001$ vs Chow-PCSK9-AAV 17 wks; ## $p<0.01$ vs DIO-PCSK9-AAV 12 wks (Dunnett`s multiple comparisons test).

3 3D imaging pipeline for aortic plaque analysis

- Vasculature dissection and fixation
- Whole aorta immunohistochemistry for CD45+ leukocytes
- Sample clearing
- Light sheet fluorescence microscopy
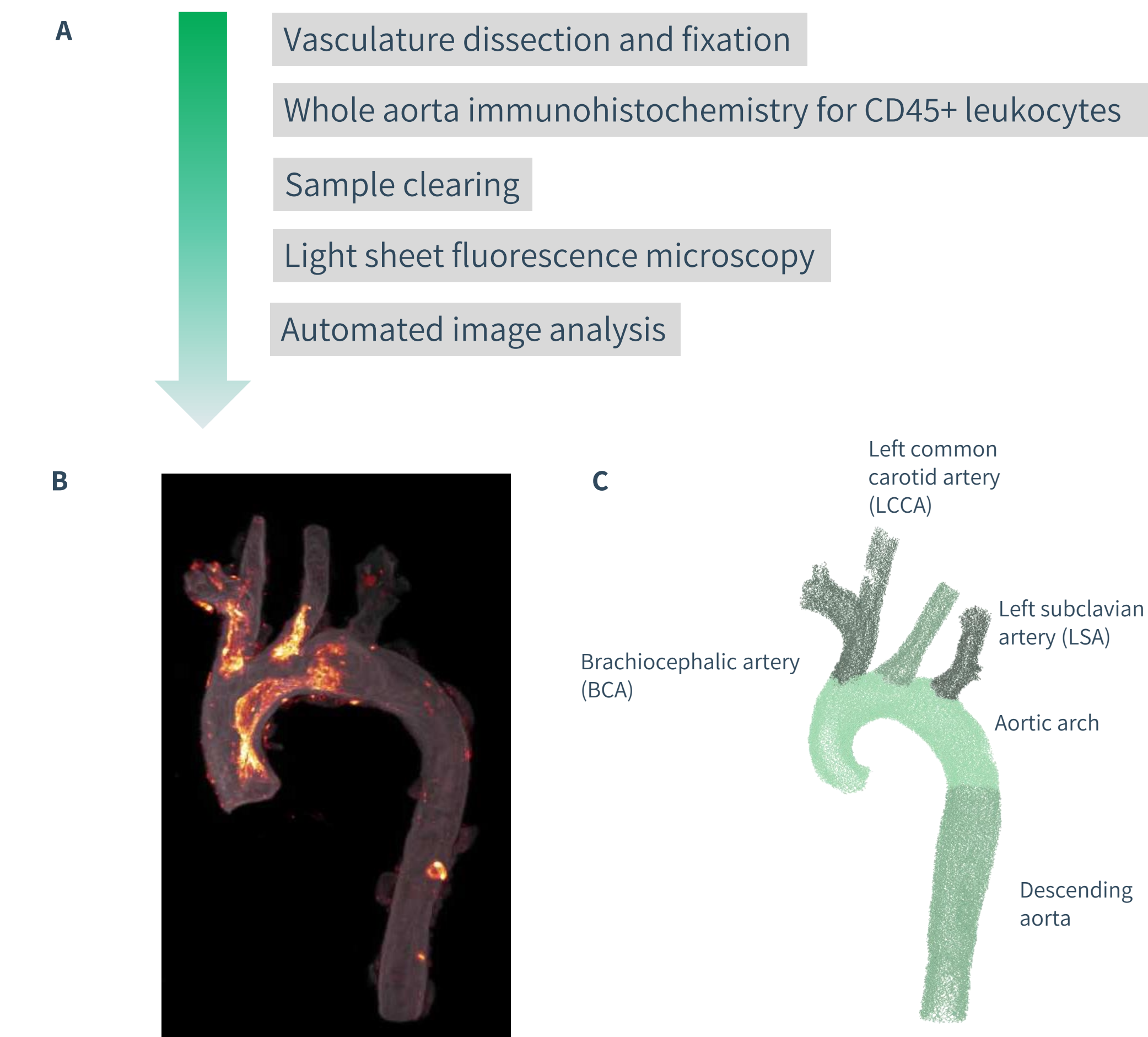- Automated image analysis

Figure 2. 3D imaging pipeline for mapping and quantification of aortic atherogenic plaque deposition. (A) Schematic overview of atherosclerosis analysis process. (B) Light sheet microscopy-imaged whole-mount aortic branch in DIO-PCSK9-AAV mouse. Tissue autofluorescence (grey), CD45-labelled leukocytes (glow scale). (C) Illustration of anatomical segmentation of individual vascular branches via light sheet microscopy data.

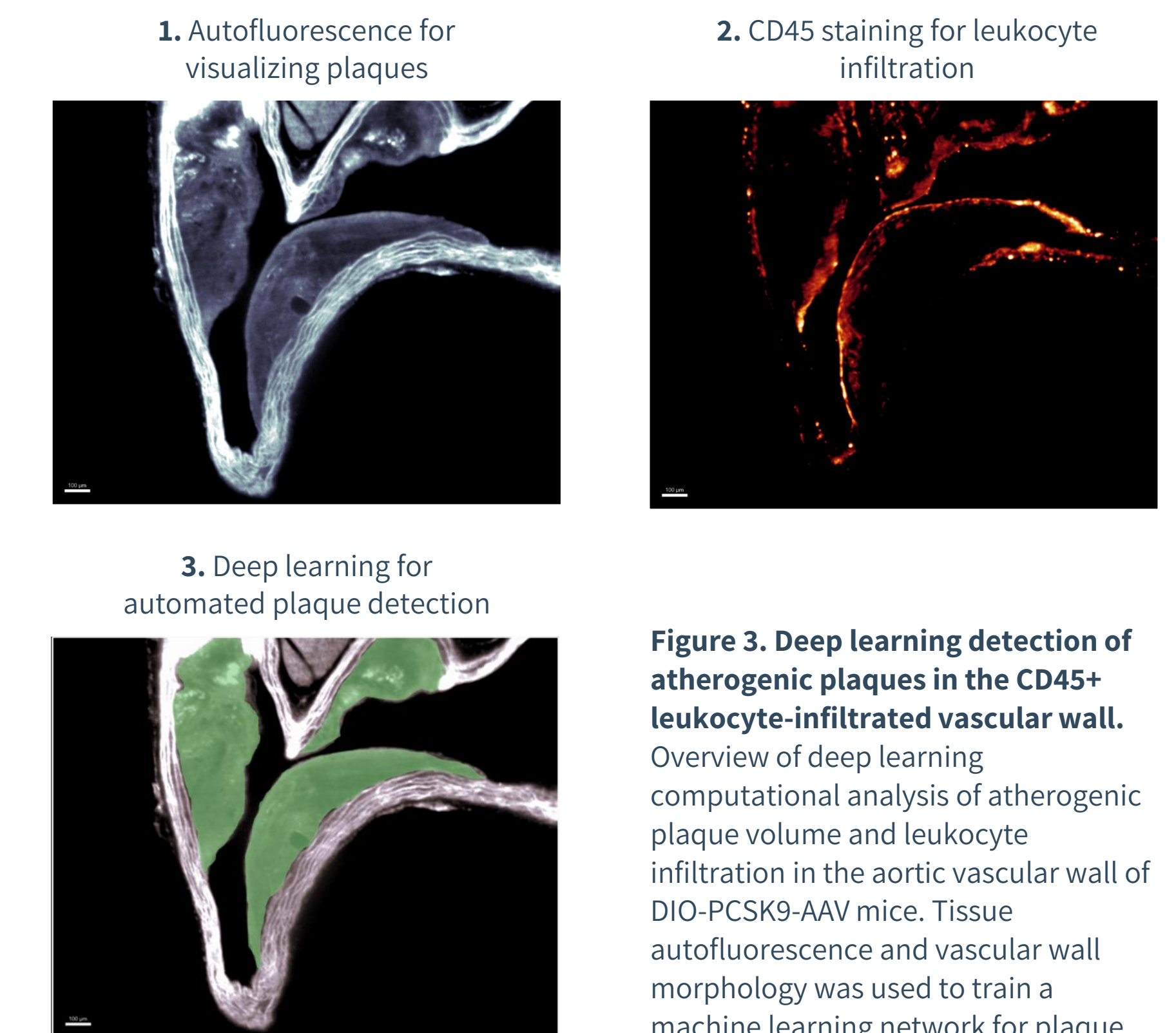## 4 AI-based detection of aortic plaques

Figure 3. Deep learning detection of atherogenic plaques in the CD45+ leukocyte-infiltrated vascular wall. Overview of deep learning computational analysis of atherogenic plaque volume and leukocyte infiltration in the aortic vascular wall of DIO-PCSK9-AAV mice. Tissue autofluorescence and vascular wall morphology was used to train a machine learning network for plaque identification.
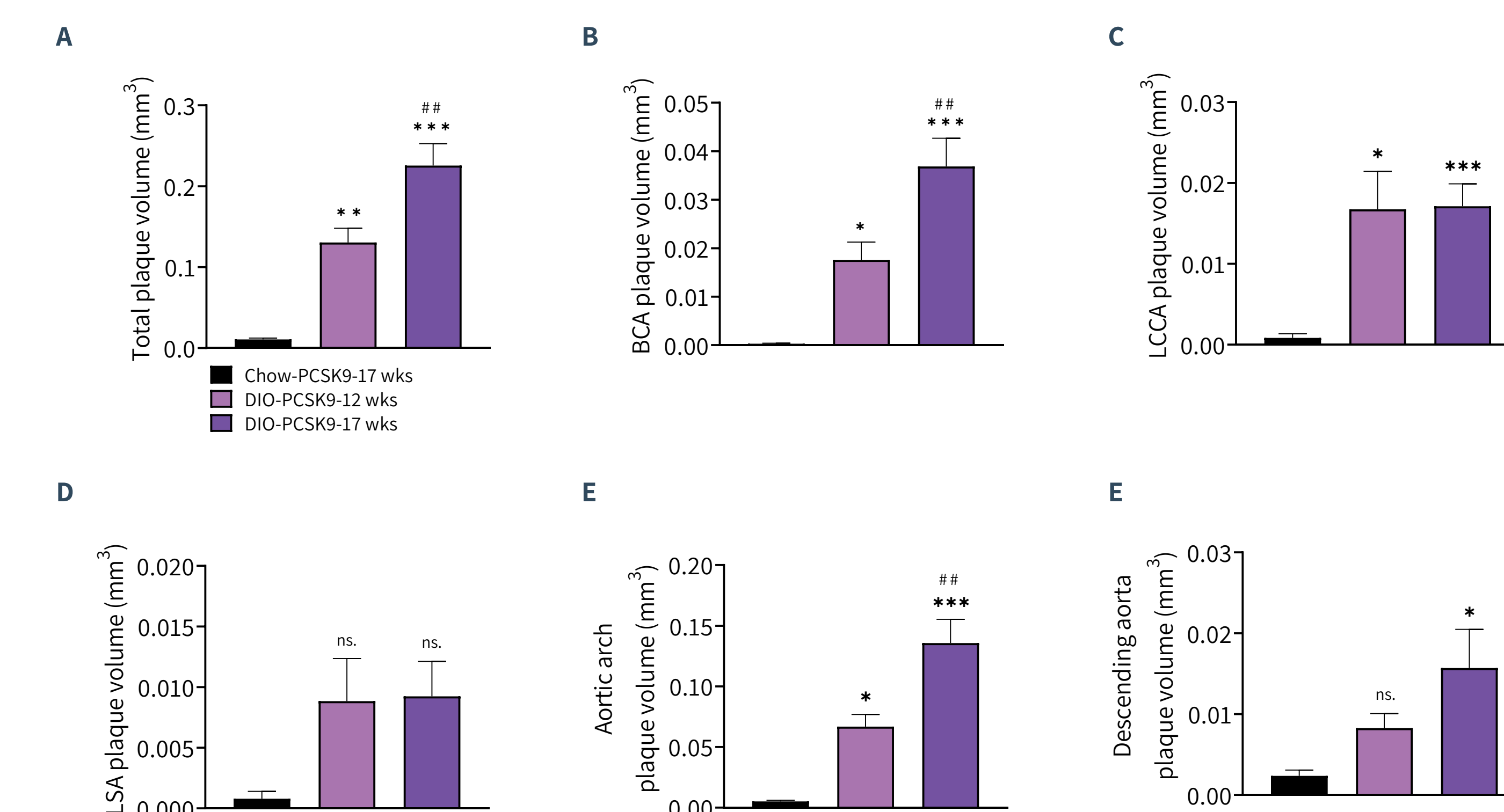
5 Aortic plaque load

Figure 4. DIO-PCSK9-AAV mice develop marked and progressive aortic plaque load. (A) Total plaque volume in the aorta. Plaque volume in the (B) brachiocephalic artery (BCA), (C) left common carotid artery (LCCA), (D) left subclavian artery (LSA), (E) aortic arch, (F) descending aorta. *$p<0.05$, **$p<0.01$, ***$p<0.001$ vs Chow-PCSK9-AAV 17 wks; ##$p<0.01$ vs DIO-PCSK9-AAV 12 wks; ns, not significant (Dunnett`s multiple comparisons test).

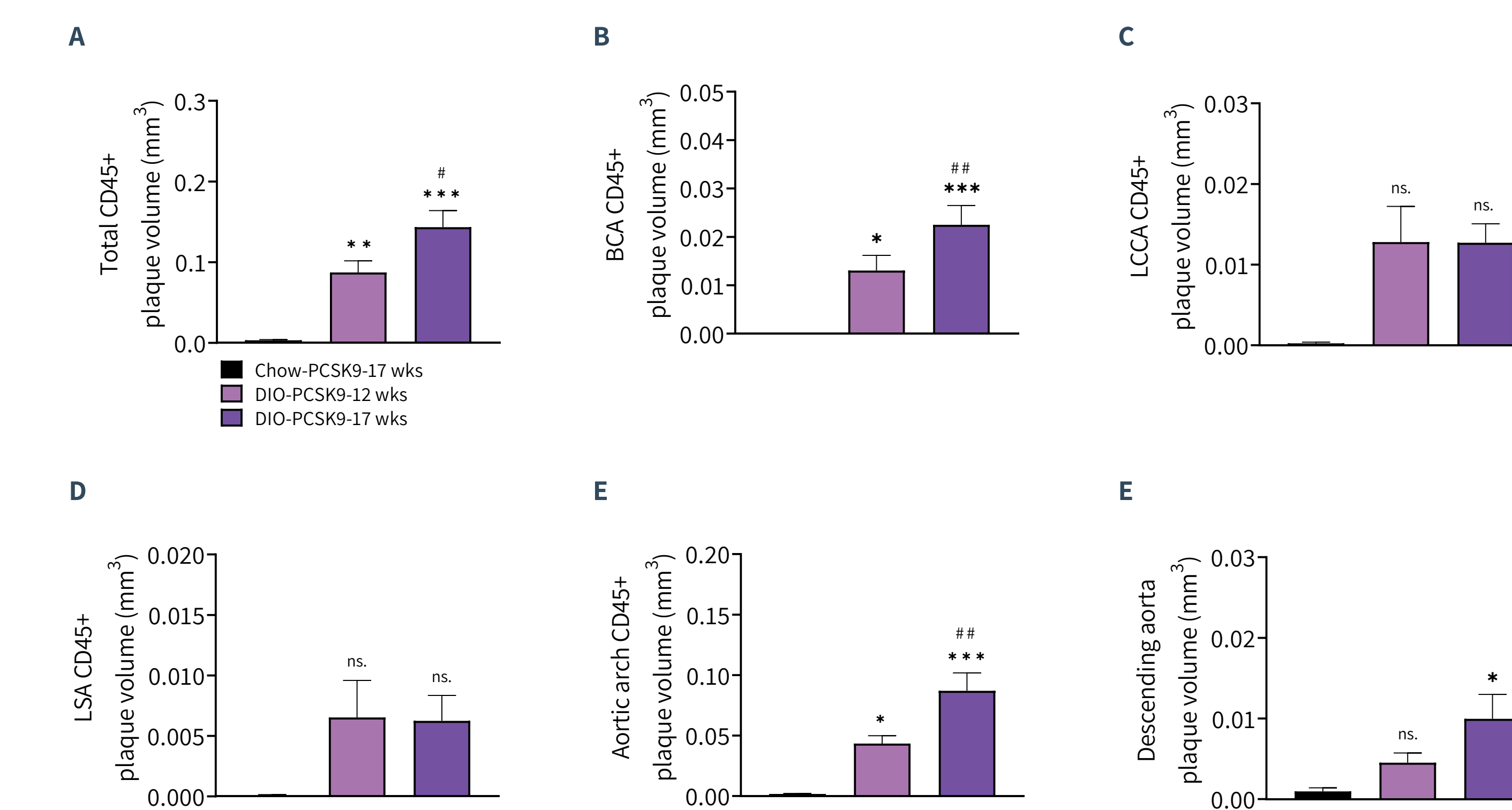## 6 CD45+ leukocyte-associated aortic plaque load

Figure 5. DIO-PCSK9-AAV mice develop marked and progressive aortic inflammatory plaque load. (A) Total plaque CD45+ immunofluorescence volume in the aorta. Plaque CD45+ immunofluorescence volume in the (B) brachiocephalic artery (BCA), (C) left common carotid artery (LCCA), (D) left subclavian artery (LSA), (E) aortic arch, (F) descending aorta. *$p<0.05$, **$p<0.01$, ***$p<0.001$ vs Chow-PCSK9-AAV 17 wks; #$p<0.05$, ##$p<0.01$ vs DIO-PCSK9-AAV 12 wks;; ns, not significant (Dunnett`s multiple comparisons test).

CONCLUSION

+ High-throughput, automated 3D light sheet imaging enables accurate volumetric assessment of aortic atherogenic plaque and inflammation load in chow-fed PSCK9-AAV mice

+ DIO-PCSK9-AAV mice demonstrate obesity with marked LDL-hypercholesterolemia and substantial increases in atherogenic plaque load in almost all aortic compartments

+ DIO-PCSK9-AAV mice demonstrate marked increases in leukocyte-associated plaque load in most aortic compartments investigated

The DIO-PSCK9-AAV mouse represents a translational model for evaluating drug effects on clinical hallmarks of dyslipidemia and atherosclerosis

Scan the QR code to learn more about our services within cardiovascular diseases.